COMMUNICATION

Selective treatment of intracellular bacterial infections using host cell-targeted bioorthogonal nanozymes†

Joseph Hardie, Jessa Marie Makabenta, [ID] Aarohi Gupta, [ID] Rui Huang, [ID] Roberto Cao-Milán, Ritabrita Goswami, Xianzhi Zhang, Parvati Abdulpurkar, Michelle E. Farkas [ID] and Vincent M. Rotello [ID] *

Intracellular bacterial infections are difficult to treat, and in the case of *Salmonella* and related infections, can be life threatening. Antibiotic treatments for intracellular infections face challenges including cell penetration and intracellular degradation that both reduce antibiotic efficacy. Even when treatable, the increased dose of antibiotics required to counter infections can strongly impact the microbiome, compromising the native roles of beneficial non-pathogenic species. Bioorthogonal catalysis provides a new tool to combat intracellular infections. Catalysts embedded in the monolayers of gold nanoparticles (nanozymes) bioorthogonally convert inert antibiotic prodrugs (pro-antibiotics) into active species within resident macrophages. Targeted nanozyme delivery to macrophages was achieved through mannose conjugation and subsequent uptake *via* the mannose receptor (CD206). These nanozymes efficiently converted pro-ciprofloxacin to ciprofloxacin inside the macrophages, selectively killing pathogenic *Salmonella enterica* subsp. *enterica* serovar Typhimurium relative to non-pathogenic *Lactobacillus* sp. in a transwell co-culture model. Overall, this targeted bioorthogonal nanozyme strategy presents an effective treatment for intracellular infections, including typhoid and tuberculosis.

Salmonella is a Gram-negative intracellular pathogen that causes systemic infections such as typhoid fever and gastroenteritis. As one of the most common sources of foodborne illness, *Salmonella* pathogens remain a threat to public health worldwide,[1] with ~1.3 billion cases of *Salmonella*-related illness and ~370 000 deaths reported every year.[2] One of the major challenges in treating *Salmonella* infections is that this pathogen invades and resides within the host's own cells, including dendritic cells, epithelial cells

Department of Chemistry, University of Massachusetts Amherst, 710 North Pleasant Street, Amherst, MA 01003, USA. E-mail: rotello@chem.umass.edu

New concepts

In intracellular infections, bacterial pathogens use the host cell as a reservoir and for protection against therapeutics, resulting in persistent and refractory infections. Since most antibiotics cannot effectively penetrate and/or accumulate inside eukaryotic cells, treatment of intracellular infections presents a daunting challenge. In this work, bioorthogonal catalysis was leveraged to generate antibiotics within host macrophages (*in situ*) to fight intracellular infections. Functionalization of iron tetraphenylporphyin-loaded gold nanoparticle nanozymes (NZs) with mannose (Man-NZs) resulted in efficient and selective uptake by macrophages, producing a localized drug "nano-factory". This platform effectively combats intracellular bacteria without adversely affecting host cells and the surrounding microbiome.

and macrophages. Macrophage invasion allows *Salmonella* to establish systemic disease in a susceptible host.[3,4] The ability of these and other pathogens to hide inside of host cells protects them from both host immune defences and antimicrobial therapeutics. These intracellular infection mechanisms can result in acute life-threatening infections and long-term, recurring chronic infections that are difficult to treat.[4,5]

Traditional antibiotic therapeutic strategies have limited efficacy against intracellular pathogens. Most antibiotics are not designed to penetrate mammalian cell membranes, and/or are degraded by enzymes in the cytosol.[6,7] As a result, high doses of antibiotics are required to kill intracellular pathogens, which magnifies their off-target effects on the microbiome.[8] Broad spectrum antibiotics eliminate both pathogenic and beneficial bacteria, attenuating the positive roles the microbiome plays in fighting infections,[9] while also generating resistant strains that lead to reduced drug efficacy.[10] Moreover, loss of a healthy microbiome leads to a range of gastrointestinal problems, in particular *C. difficile* infection.[11,12] These challenges are all exacerbated by a lack of progress in the development of new antibiotics, making it unlikely that a new drug effective against intracellular infections will be available soon.[13]

Localization of therapeutic activity to affected host cells is a key challenge in treating intracellular infections.[14] Bioorthogonal transition metal catalysts (TMCs) provide a strategy for on-demand generation of therapeutics at the infection site. However, their direct utilization poses significant challenges as they have limited solubility in aqueous conditions and are prone to deactivation in biological systems.[15,16] Integrating TMCs with nanoparticles provide bioorthogonal 'nanozymes' (NZ) to produce drugs and imaging agents in complex biosystems *in situ*,[17,18] differentiating them from commonly used nanozymes with intrinsic peroxidase-mimicking activity.[19–21]

We report here the fabrication of a targeted nanozyme that converts pro-antibiotics into antibiotics inside cells to effectively eradicate intracellular pathogenic bacteria. Here, we have generated negatively charged nanozymes functionalized with mannose (Man-NZ) that are efficiently and selectively internalized by macrophages. These nanozymes consist of mannose-functionalized gold nanoparticle scaffolds (2 nm core, Man-AuNPs), with iron tetraphenylporphyin (FeTPP) serving as a bioorthogonal catalyst.[22] Mannose functionalization allows specific binding to the mannose receptor (CD206) present on the surface of macrophages,[23,24] facilitating selective uptake of Man-NZ. Once internalized, Man-NZ efficiently converts a phenylazide-caged pro-ciprofloxacin into ciprofloxacin to specifically kill pathogenic *Salmonella* (Fig. 1). Transwell co-culture studies using *Salmonella*-infected macrophages and non-pathogenic *Lactobacillus* species bacteria indicated that antibiotic activity was localized within the macrophages. Intracellular *Salmonella* levels were reduced significantly, and minimal toxicity to *Lactobacillus* sp. was observed. Taken together, this nanozyme strategy combines ligand-receptor targeting with bioorthogonal catalysis to create an effective, site-specific intracellular antibiotic treatment that concurrently minimizes off-target toxicity.

Gold nanoparticles (AuNPs) are established as safe for therapeutic delivery and feature facile synthesis and functionalization.[25,26] Negatively charged gold nanoparticles (COOH-AuNPs) featuring biocompatible tetra(ethylene)glycol spacers and carboxylate headgroups were used to minimize non-specific uptake of the nanozyme.[27] These particles were synthesized from pentanethiol-capped 2 nm core AuNPs using a place exchange reaction, as previously reported.[17] The particles were then post-functionalized *via* EDC (1-ethyl-3-(3-dimethylaminopropyl)-carbodiimide)/NHS(*N*-hydroxy sulfosuccinimide) coupling with D-mannosamine to display mannose moieties for macrophage targeting. The density of D-mannose ligands on Man-AuNPs was quantified using an anthrone/sulfuric acid assay[28,29] that has been used for quantitative analysis of carbohydrates in glyconanoparticle analysis (Fig. S1, ESI†).[30–32] The surface coverage was determined to be ~40% (see ESI† for calculation details). Zeta potential values were consistent with these measurements, shifting from
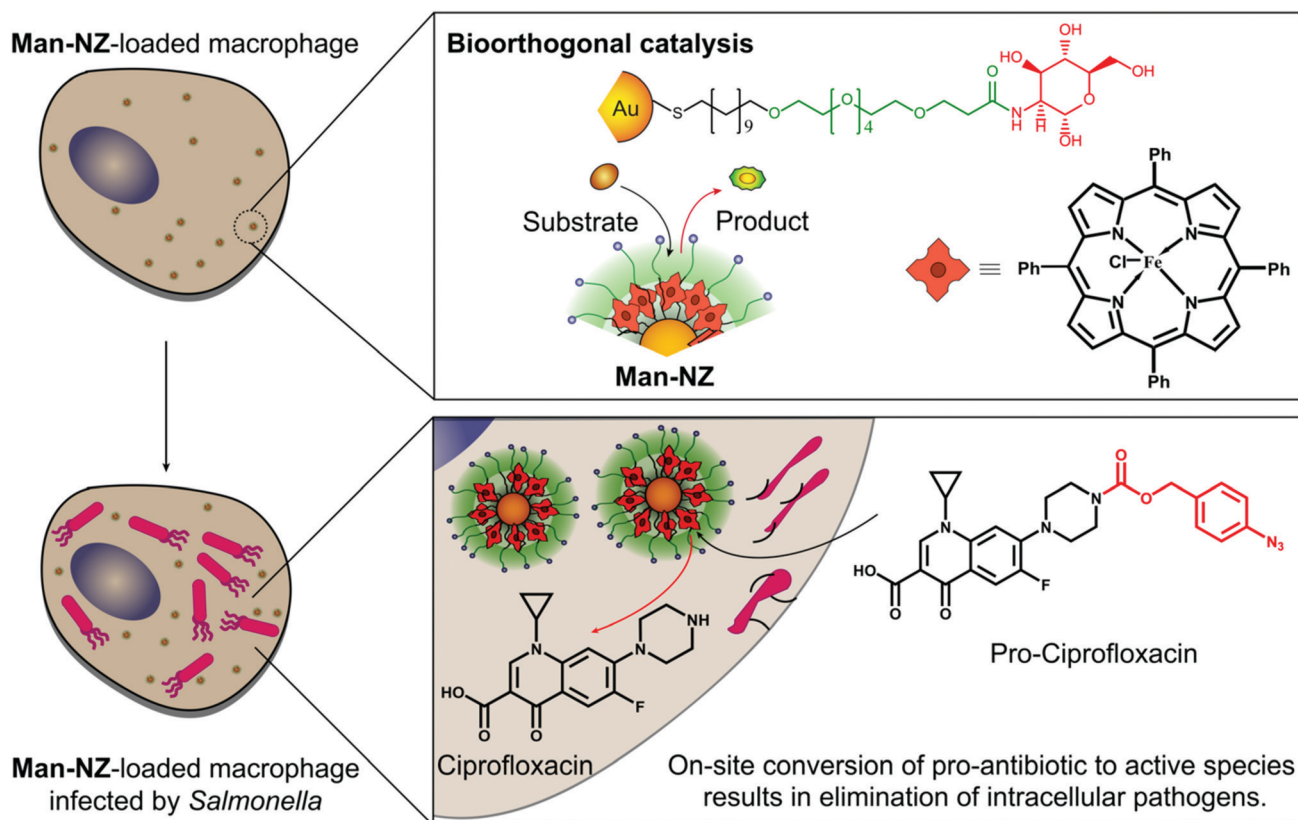

Fig. 1 Macrophage uptake of mannose–targeted nanozymes (Man-NZ) followed by administration of a bioorthogonally-caged prodrug generates antibiotics inside cells.

−42.7 mV to −7.9 mV after mannose conjugation (Fig. S2, ESI†). Significantly, the **Man-AuNPs** retained a negative charge, enabling the minimization of non-specific uptake. Further characterization of both **AuNPs** and **Man-AuNPs** was performed through dynamic light scattering (DLS) measurement and transmission electron microscopy (TEM) (Fig. S3 and S4, ESI†).

Mannose nanozymes (**Man-NZs**) were fabricated by encapsulating 5,10,15,20-tetraphenyl-21*H*,23*H*-porphine (**TPP**)-iron(III) complexes (**FeTPP**) into **Man-AuNP** scaffolds. The **FeTPP** molecule catalyzes the reduction of aryl azides to corresponding amines[22] and has been used as an efficient bioorthogonal catalyst.[33,34] **Man-NZs** were prepared by mixing an aqueous solution of **Man-AuNPs** with **FeTPP** dissolved in tetrahydrofuran (THF) and stirring for 10 min. Evaporation of THF drives encapsulation of the catalyst into the hydrophobic pockets of **Man-AuNPs**. The amount of **FeTPP** encapsulated in **Man-AuNPs** was determined quantitatively using ICP-MS analysis (Fig. 2a and Fig. S5, ESI†). Afterwards, the catalytic properties of the nanozymes were demonstrated through efficient uncaging of a non-fluorescent resorufin-based profluorophore (**pro-res**),[33,34] where **FeTPP** catalytically reduces the azide, resulting in fragmentation that releases the fluorescent resorufin molecule (Fig. 2b-c).[35,36] **Man-AuNPs** alone do not contribute to the catalytic activation of the **Pro-Res**.

After generating the nanozyme, the selective uptake of **Man-NZ** by macrophages was quantified using ICP-MS (Fig. 3 and Fig. S6, S7, ESI†). As expected, **Man-NZ** was internalized by RAW 264.7 macrophages in a dose-dependent fashion and was retained even after 72 hours (Fig. S7, ESI†). In contrast, **Man-NZ** was not internalized by HepG2 hepatocytes, even at the highest dose, due to its negative charge. Significantly higher levels of macrophage uptake were observed for the targeted **Man-NZ** relative to the untargeted **COOH-NZ** (Fig. 3a). This selective uptake by macrophages over HepG2 also indicates expected safety of the platform towards healthy liver cells.[37,38] Moreover, M2 phenotype macrophages (*i.e.*, stimulated by IL-4) displayed higher uptake compared to those of M0 and M1 phenotype (Fig. 3b and Fig. S7b, ESI†), further confirming the mannose receptor-based targeting by our nanozyme system (M2-polarized macrophages possess increased CD206). For M2 phenotype cells, **Man-NZ** has substantially greater uptake than **COOH-NZ** (Fig. 3c). **Man-NZ** was non-toxic to the macrophages even at high concentrations, as demonstrated by Alamar Blue assay (Fig. S8, ESI†).

The intracellular activity of **Man-NZ** was demonstrated by activation of non-fluorescent **pro-res**. Non-polarized macrophage cells were incubated with **Man-NZ** overnight, washed, and then the pro-fluorophore was added and incubated for an additional 2 h followed by washing (Fig. 4). Confocal microscopy imaging revealed that cells treated with both **Man-NZ** and **pro-res** had noticeably more intense red fluorescence than cells treated with **pro-res** or **Man-NZ** alone. Significantly, cellular fluorescence was observed to be distributed throughout the cytosol, a prerequisite for addressing intracellular infections.

After confirming the activity of the **Man-NZ** inside macrophages, we next assessed the therapeutic efficacy of the
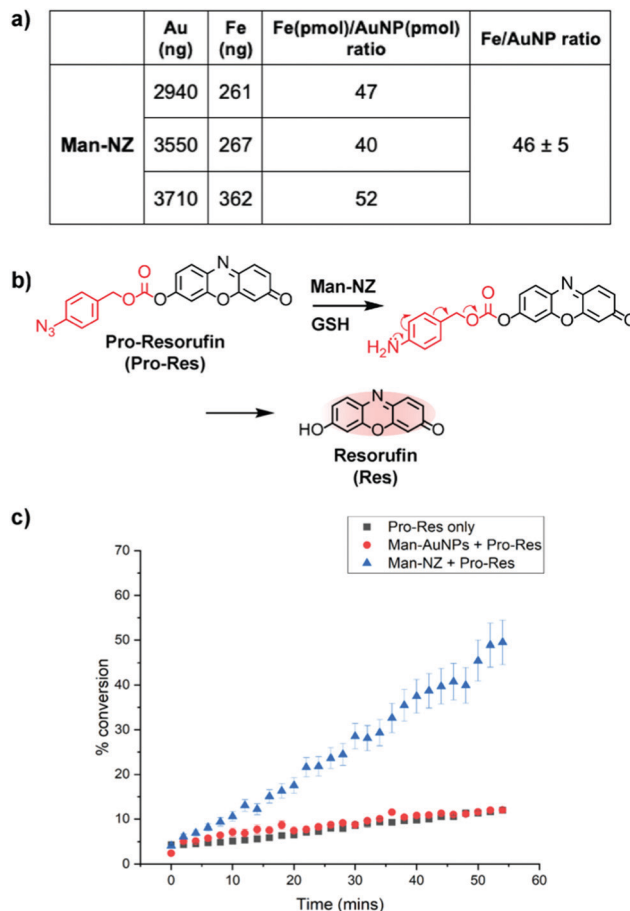
Fig. 2 (a) ICP-MS quantification of **FeTPP** catalyst loading in **Man-NZ** based on results from Fig. S5 (ESI†); (b) activation of pro-resorufin to red fluorescent resorufin by **Man-NZ**; glutathione (GSH) was used as the cofactor; (c) percent conversion of 20 μM pro-resorufin into resorufin over time by 500 nM **Man-NZ** or **Man-AuNPs**, with 5 mM GSH as cofactor. **Pro-res** only served as control. Error bars represent standard deviation ($n = 3$).

nanozyme strategy using pro-antibiotics. We synthesized an azidophenyl-caged ciprofloxacin (pro-ciprofloxacin; **pro-cip**)[34] that is converted to the active antibiotic, ciprofloxacin, by **Man-NZ** (Fig. 1 and Fig. S9, ESI†). This system was tested against the causative pathogen for typhoid, *Salmonella enterica* subsp. *enterica* serovar Typhimurium (Fig. 5a). Treatment of planktonic bacteria with both **Man-NZ** and **pro-cip** resulted in an approximately 4 log reduction of *Salmonella* colony forming units (CFUs), similar to the activity of ciprofloxacin. Groups treated with **pro-cip** only or **Man-NZ** only resulted in no significant *Salmonella* reduction compared to the untreated [phosphate buffered saline (PBS) only] control group, demonstrating that activity arises from effective bioorthogonal catalysis by **Man-NZ**.

Following confirmation of antibiotic activation through killing of planktonic bacteria, we determined the efficacy of the **Man-NZ** + **pro-cip** system in an intracellular macrophage *Salmonella* infection model.[39] In brief, RAW 264.7 macrophages were seeded in a 96-well plate, then treated with **Man-NZ**
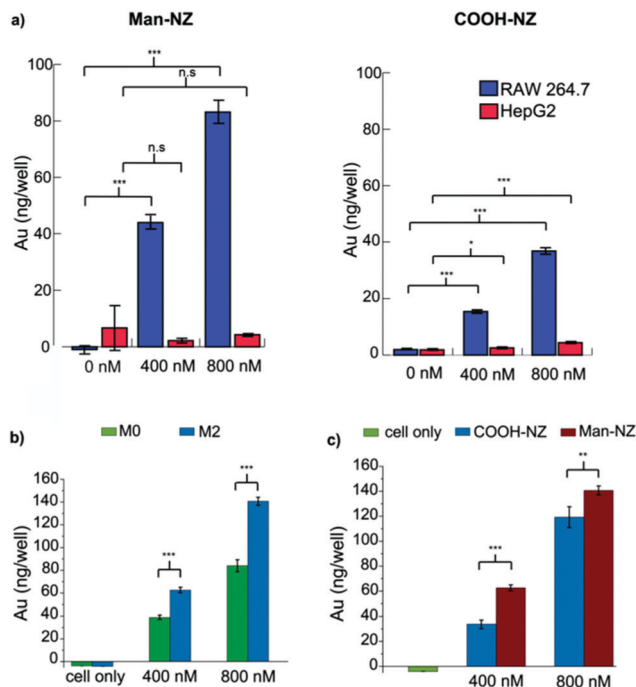
Fig. 3   ICP-MS analysis of gold accumulation in (a) RAW 264.7 macrophages and HepG2 hepatocytes following 24 h incubation with varying concentrations of **Man-NZ** (left) and **COOH-NZ** control (right); (b) M0 and M2 phenotype RAW 264.7 macrophages following 24 h incubation with **Man-NZ**; and (c) M2 phenotype RAW 264.7 macrophages following 24 h incubation of **COOH-NZ** and **Man-NZ**. The M2 phenotype was stimulated by IL-4. Error bars represent standard deviation (n = 3). *, **, *** = P values < 0.05, 0.01, 0.001, respectively.
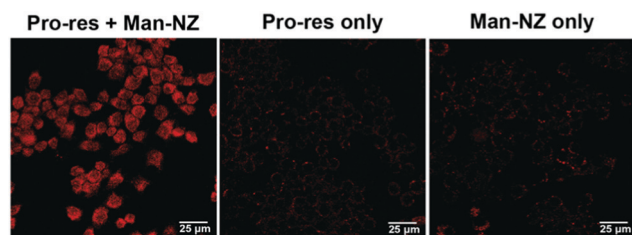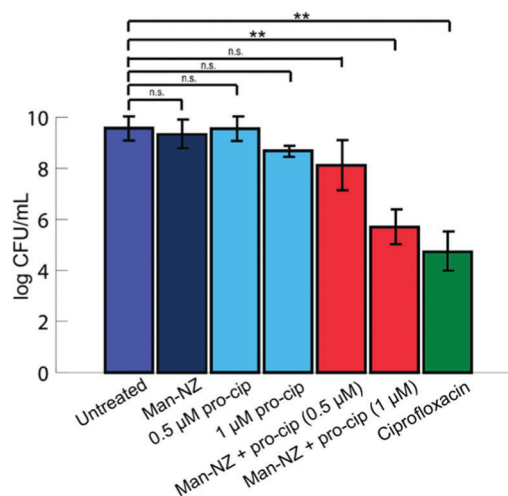

Fig. 4   Confocal images of non-polarized RAW 264.7 macrophages incubated with **Man-NZ** overnight and then with **pro-res** for 2h (left). Macrophages treated with **pro-res** only (middle) and **Man-NZ** only (right) served as controls.
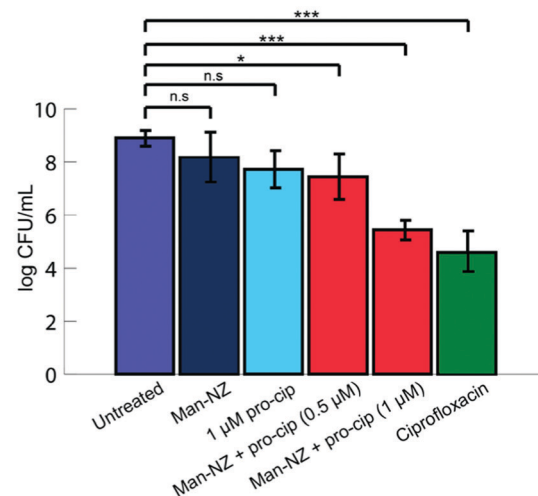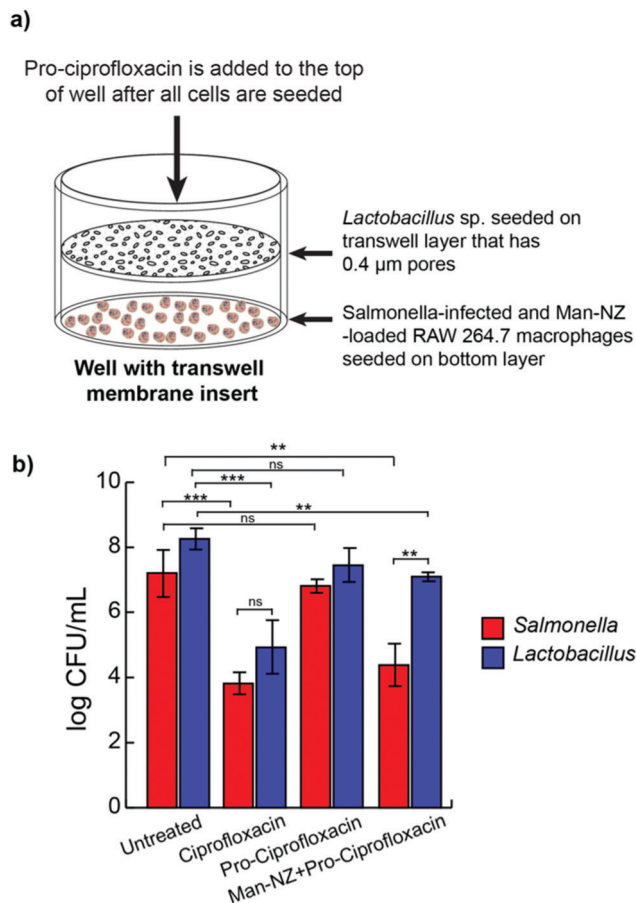

Fig. 5   (a) Viability of *Salmonella* after 24 hr treatment with pro-ciprofloxacin and **Man-NZ**, compared to controls, as determined by quantitative colony counting. (b) Viability of *Salmonella* residing inside macrophages after 24 hr treatment with **pro-cip** and **Man-NZ** or controls, as determined by quantitative colony counting in a *Salmonella*-macrophage infection model. Data are presented as mean ± standard deviation, n = 3 (*, **, *** = P values < 0.05, 0.01, 0.001, respectively).

overnight to facilitate uptake. Following, macrophages were infected by incubating the cells with *Salmonella* (1 : 100 multiplicity of infection) for an hour. The macrophages were then washed and incubated with gentamicin for 30 minutes to remove extracellular bacteria. Afterwards, pro-ciprofloxacin was added. The macrophages were then lysed and the surviving bacteria were collected and quantified through CFU counting. Treatment with **Man-NZ** + **pro-cip** reduced intracellular bacterial CFUs to a similar extent as ciprofloxacin did (Fig. 5b). Importantly, concentrations of **pro-cip**, ciprofloxacin, and **Man-NZ** + **pro-cip** used in this study were confirmed to be

non-toxic to the macrophages by Alamar Blue assay (Fig. S10 and S11, ESI†). Treatment with **Man-NZ** only or pro-ciprofloxacin only did not significantly reduce *Salmonella* CFUs, demonstrating the ability of the **Man-NZ** to generate active antibiotics inside macrophages for killing of intracellular pathogenic bacteria. This activity was further validated in an additional murine macrophage type, J744 (Fig. S12a, ESI†). We also tested our strategy using methicillin-resistant *Staphylococcus aureus* (MRSA)-infected RAW 264.7 macrophages; MRSA is another prevalent intracellular pathogen. As before, treatment with **Man-NZ** + **pro-cip** resulted in reduction of intracellular bacteria viability, comparable to the activity of the active drug (Fig. S12b, ESI†).

Fig. 6 (a) Schematic of transwell co-culture assay with *Salmonella*-infected, **Man-NZ**-loaded macrophages and *Lactobacillus*. (b) Viability of *Lactobacillus* sp. and intracellular *Salmonella* after 24 h treatment with pro-ciprofloxacin and **Man-NZ**, and controls in a transwell co-culture model as determined by quantitative colony counting. Data are presented as mean $\pm$ standard deviation, n = 3. *, **, *** = P values < 0.05, 0.01, 0.001, respectively.

Traditional antibiotic therapies for intestinal infections generally result in a substantial reduction of beneficial gut bacteria,[9,40] leading to an array of indirect effects.[8,41] We hypothesized that generation of antibiotics inside of macrophages would result in higher local concentrations of therapeutics. As a result, the *in situ* generation of antibiotics would allow lower overall dosing, minimizing effects on the surrounding microbiome. To test this possibility, we developed a transwell membrane model in which *Lactobacillus* species, a dominant organism in the human gut, was co-cultured with *Salmonella*-infected RAW 264.7 macrophages (Fig. 6a). Briefly, **Man-NZ**-loaded macrophages were plated at the bottom of a well and infected with *Salmonella*, while *Lactobacillus* sp. (BioK⁺) were added to the transwell membrane (0.4 μm pore size). Pro-ciprofloxacin or ciprofloxacin was then added to the top of the well. Quantitative colony counting after 24 h of treatment revealed that pro-ciprofloxacin treatment of **Man-NZ**-loaded macrophages resulted in significant *Salmonella* colony reduction (>3 log units) while *Lactobacillus* CFUs were

minimally affected (<1 log unit; Fig. 6b and Fig. S13, ESI†). In contrast, traditional ciprofloxacin treatment killed both *Salmonella* and *Lactobacillus* to significant extents, as expected due to the broad-spectrum activity of the antibiotic. As in the previous experiments, the pro-ciprofloxacin alone control did not affect CFU counts of either bacteria type. Taken together, this study demonstrates the strong potential of nanozyme-based systems to treat intracellular infections while maintaining overall gut microbiome diversity.

Conclusions

In summary, we have generated macrophage-targeted bioorthogonal nanozymes to produce antibiotics at the sites of intracellular bacterial infections. Negatively charged nanozymes post-functionalized with a mannose terminal headgroup demonstrated high selectivity for uptake by macrophages. Following internalization, the nanozyme retained its catalytic activity as demonstrated by the conversion of non-fluorescent pro-resorufin into the fluorescent resorufin. Activation of pro-ciprofloxacin by **Man-NZ** inside of *Salmonella*-infected macrophages resulted in effective killing of intracellular *Salmonella*. The ability to generate effective concentrations of antibiotic inside of the macrophages provides high selectivity for intracellular infections and an important new strategy for treatment of these infections without harming the surrounding microbiome. This bioorthogonal approach has the potential to effectively treat intracellular infections ranging from typhoid to tuberculosis – diseases that affect millions globally every year.

Author contributions

The manuscript was written through contributions of all authors. All authors have given approval to the final version of the manuscript.

Conflicts of interest

There are no conflicts to declare.

Acknowledgements

References

1 T. Pang, Z. A. Bhutta, B. B. Finlay and M. Altwegg, *Trends Microbiol.*, 1995, **3**, 253–255.

2 P. J. Dodd, C. M. Yuen, C. Sismanidis, J. A. Seddon and H. E. Jenkins, *Lancet Global Health*, 2017, **5**, e898–e906.

3 D. M. Monack, B. Raupach, A. E. Hromockyj and S. Falkow, *Proc. Natl. Acad. Sci. U. S. A.*, 1996, **93**, 9833–9838.

4 L. Jiang, P. Wang, X. Song, H. Zhang, S. Ma, J. Wang, W. Li, R. Lv, X. Liu, S. Ma, J. Yan, H. Zhou, D. Huang, Z. Cheng, C. Yang, L. Feng and L. Wang, *Nat. Commun.*, 2021, **12**, 879.

5 Y. Li, Y. Liu, Y. Ren, L. Su, A. Li, Y. An, V. Rotello, Z. Zhang, Y. Wang, Y. Liu, S. Liu, J. Liu, J. D. Laman, L. Shi, H. C. van der Mei and H. J. Busscher, *Adv. Funct. Mater.*, 2020, **30**, 202004942.

6 P. M. Tulkens, *Eur. J. Clin. Microbiol. Infect. Dis.*, 1991, **10**, 100–106.

7 L. Jiang, M. K. Greene, J. L. Insua, J. S. Pessoa, D. M. Small, P. Smyth, A. P. McCann, F. Cogo, J. A. Bengoechea, C. C. Taggart and C. J. Scott, *J. Controlled Release*, 2018, **279**, 316–325.

8 B. P. Willing, S. L. Russell and B. B. Finlay, *Nat. Rev. Microbiol.*, 2011, **9**, 233–243.

9 M. Blaser, *Nature*, 2011, **476**, 393–394.

10 J. M. A. Blair, M. A. Webber, A. J. Baylay, D. O. Ogbolu and L. J. V. Piddock, *Nat. Rev. Microbiol.*, 2015, **13**, 42–51.

11 C. Jernberg, S. Löfmark, C. Edlund and J. K. Jansson, *Microbiology*, 2010, **156**, 3216–3223.

12 C. P. Kelly and J. T. Lamont, *Annu. Rev. Med.*, 1998, **49**, 375–390.

13 World Health Organization, 2019 *Antibacterial agents in clinical development: an analysis of the antibacterial clinical development pipeline. Geneva: World Health Organization; 2019. Licence: CC BY-NC-SA 3.0 IGO.*, 2019.

14 J. M. V. Makabenta, A. Nabawy, C. H. Li, S. Schmidt-Malan, R. Patel and V. M. Rotello, *Nat. Rev. Microbiol.*, 2021, **19**, 23–36.

15 T. Völker, F. Dempwolff, P. L. Graumann and E. Meggers, *Angew. Chem., Int. Ed.*, 2014, **53**, 10536–10540.

16 S. Fedeli, J. Im, S. Gopalakrishnan, J. L. Elia, A. Gupta, D. Kim and V. M. Rotello, *Chem. Soc. Rev.*, 2021, **50**, 13467–13480.

17 G. Y. Tonga, Y. Jeong, B. Duncan, T. Mizuhara, R. Mout, R. Das, S. T. Kim, Y. C. Yeh, B. Yan, S. Hou and V. M. Rotello, *Nat. Chem.*, 2015, **7**, 597–603.

18 R. Das, R. F. Landis, G. Y. Tonga, R. Cao-Milán, D. C. Luther and V. M. Rotello, *ACS Nano*, 2019, **13**, 229–235.

19 M. Liang and X. Yan, *Acc. Chem. Res.*, 2019, **52**, 2190–2200.

20 Q. Liang, J. Xi, X. J. Gao, R. Zhang, Y. Yang, X. Gao, X. Yan, L. Gao and K. Fan, *Nano Today*, 2020, **35**, 100935.

21 Y. Hao, Y. Chen, X. He, Y. Yu, R. Han, Y. Li, C. Yang, D. Hu and Z. Qian, *Adv. Sci.*, 2020, **7**, 2001853.

22 P. K. Sasmal, S. Carregal-Romero, A. A. Han, C. N. Streu, Z. Lin, K. Namikawa, S. L. Elliott, R. W. Köster, W. J. Parak and E. Meggers, *ChemBioChem*, 2012, **13**, 1116–1120.

23 F. Y. Su, S. Srinivasan, B. Lee, J. Chen, A. J. Convertine, T. E. West, D. M. Ratner, S. J. Skerrett and P. S. Stayton, *J. Controlled Release*, 2018, **287**, 1–11.

24 J. Chen, F. Y. Su, D. Das, S. Srinivasan, H. N. Son, B. Lee, F. Radella, D. Whittington, T. Monroe-Jones, T. E. West, A. J. Convertine, S. J. Skerrett, P. S. Stayton and D. M. Ratner, *Biomaterials*, 2019, **195**, 38–50.

25 S. Rana, A. Bajaj, R. Mout and V. M. Rotello, *Adv. Drug Delivery Rev.*, 2012, **64**, 200–216.

26 E. E. Connor, J. Mwamuka, A. Gole, C. J. Murphy and M. D. Wyatt, *Small*, 2005, **1**, 325–327.

27 Y. Jiang, S. Huo, T. Mizuhara, R. Das, Y. W. Lee, S. Hou, D. F. Moyano, B. Duncan, X. J. Liang and V. M. Rotello, *ACS Nano*, 2015, **9**, 9986–9993.

28 A. Leyva, A. Quintana, M. Sánchez, E. N. Rodríguez, J. Cremata and J. C. Sánchez, *Biologicals*, 2008, **36**, 134–141.

29 X. Wang, O. Ramström and M. Yan, *J. Mater. Chem.*, 2009, **19**, 8944–8949.

30 A. A. Kulkarni, C. Fuller, H. Korman, A. A. Weiss and S. S. Iyer, *Bioconjugate Chem.*, 2010, **21**, 1486–1493.

31 Y. Y. Chien, M. D. Jan, A. K. Adak, H. C. Tzeng, Y. P. Lin, Y. J. Chen, K. T. Wang, C. T. Chen, C. C. Chen and C. C. Lin, *ChemBioChem*, 2008, **9**, 1100–1109.

32 V. Ramtenki, D. Raju, U. J. Mehta, C. V. Ramana and B. L. V. Prasad, *New J. Chem.*, 2013, **37**, 3716–3720.

33 R. Cao-Milán, S. Gopalakrishnan, L. D. He, R. Huang, L. S. Wang, L. Castellanos, D. C. Luther, R. F. Landis, J. M. V. Makabenta, C. H. Li, X. Zhang, F. Scaletti, R. W. Vachet and V. M. Rotello, *Chem*, 2020, **6**, 1113–1124.

34 R. Huang, C. H. Li, R. Cao-Milán, L. D. He, J. M. Makabenta, X. Zhang, E. Yu and V. M. Rotello, *J. Am. Chem. Soc.*, 2020, **142**, 10723–10729.

35 K. Gorska, A. Manicardi, S. Barluenga and N. Winssinger, *Chem. Commun.*, 2011, **47**, 4364–4366.

36 S. Matikonda, J. M. Fairhall, F. Fiedler, S. Sanhajariya, R. A. J. Tucker, S. Hook, A. L. Garden and A. B. Gamble, *Bioconjugate Chem.*, 2018, **29**, 324–334.

37 S. G. Elci, Y. Jiang, B. Yan, S. T. Kim, K. Saha, D. F. Moyano, G. Yesilbag Tonga, L. C. Jackson, V. M. Rotello and R. Vachet, *ACS Nano*, 2016, **10**, 5536–5542.

38 S. T. Kim, K. Saha, C. Kim and V. M. Rotello, *Acc. Chem. Res.*, 2013, **46**, 681–691.

39 M. J. Ellis, C. N. Tsai, J. W. Johnson, S. French, W. Elhenawy, S. Porwollik, H. Andrews-Polymenis, M. McClelland, J. Magolan, B. K. Coombes and E. D. Brown, *Nat. Commun.*, 2019, **10**, 197.

40 C. F. A. Ribeiro, G. G. D. O. S. Silveira, E. D. S. Cândido, M. H. Cardoso, C. M. Espínola Carvalho and O. L. Franco, *ACS Infect. Dis.*, 2020, **6**, 2544–2559.

41 A. Palleja, K. H. Mikkelsen, S. K. Forslund, A. Kashani, K. H. Allin, T. Nielsen, T. H. Hansen, S. Liang, Q. Feng, C. Zhang, P. T. Pyl, L. P. Coelho, H. Yang, J. Wang, A. Typas, M. F. Nielsen, H. B. Nielsen, P. Bork, J. Wang, T. Vilsbøll, T. Hansen, F. K. Knop, M. Arumugam and O. Pedersen, *Nat. Microbiol.*, 2018, **3**, 1255–1265.